APPEARS IN SPIE 1988
VOL. 1005, OPTICS, ILLUMINATION...
MORE COMPREHENSIVE VERSION
TO APPEAR CVPR 1989

SEGMENTATION OF SPECULAR HIGHLIGHTS FROM OBJECT SURFACES

Lawrence B. Wolff[1]
Computer Science Department
Columbia University
New York, N.Y. 10027

Columbia University Technical Report CS-394-88
September 1988

ABSTRACT

A major hindrance to image segmentation tasks are the presence of specular highlights on object surfaces. Specular highlights appear on object surfaces where the specular component of reflection from illuminating light sources is so dominant that most detail of the object surface is obscured by a bright region of reflected light. Specular highlights are very common artifacts of most lighting environments and are not part of the intrinsic visible detail of an object surface. As a result, in addition to obscuring visible detail, specular highlight regions of an image can easily deceive image understanding algorithms into interpreting these regions as separate objects or regions on an object with high albedo.

Recently, a couple of approaches to identifying specular highlight regions in images of object surfaces have produced some good results using color analysis. Unfortunately these methods work only for dielectric materials (e.g. plastic, rubber etc..) and require that the color of the object be different from the color of the light source. In this paper a technique is presented exploiting the polarization properties of reflected light to identify specular highlight regions. This technique works for both dielectric and metal surfaces regardless of the color of the illuminating light source, or the color detail on the object surface. In addition to separating out diffuse and specular components of reflection, the technique presented here also as a bonus can identify whether certain image regions correspond to a dielectric or metal object surface.

Extensive experimentation will be presented for a variety of dielectric and metal surfaces, both polished and rough. Experimentation with coated surfaces using the technique presented here have not yet been studied.

1 INTRODUCTION

The problem of identifying specular highlights on an object surface can be generalized to the problem of separating the diffuse and specular reflection components at each point on an object surface. This enables

[1]This work was supported in part by ARPA grant #N00039-84-C-0165 and NSF grant IRI-88-00370. This work was supported in part by an IBM Graduate Fellowship Award.

the identification of specular highlights at regions where the specular component of reflection is high. The separation of shading and highlight components (i.e. diffuse and specular components) was first suggested in [Barrow and Tenenbaum 1978] as being useful for intensity analysis because each individual reflection component is more simply related to the illumination and viewer geometry than is the sum of the two reflection components together. This is particularly true for rough object surfaces where the specular component of reflection is expressed with respect to a microfacet distribution function which is a very complicated function of imaging geometry. Such microfacet distribution functions are presented in [Torrance and Sparrow 1967] and [Cook and Torrance 1981]. The complicated nature of specular reflection from rough surfaces makes it very difficult to implement methods such as photometric stereo, presented in [Woodham 1978], to determine local surface normals on smooth objects whose rough level of detail is within pixel resolution. Removal of the specular component of reflection from rough surfaces, leaving the diffuse component of reflection which is Lambertian in nature, makes implementation of photometric stereo feasible on these types of surfaces.

Presented in [Shafer 1985] is the *Dichromatic Reflection Model* for dielectric object surfaces which is used to separate diffuse and specular components of reflection based upon the color of the total reflected light. This model of reflection states that the color of light reflected from dielectric objects , represented as a vector in color space, is a linear combination of two color vectors; the color vector for the *body component*[2] (i.e. shading or matte reflection) and the color vector for the *interface component*[3] (i.e. highlight reflection). The color of the body component of reflection depends upon the dielectric makeup of the object material, whereas the color of the interface component is equal to the color of an illuminating light source. At specular highlights the color of the illuminant is added to the body color of the object. Experimental evidence is shown in [Klinker, Shafer and Kanade 1987] that demonstrates the separation of the body and specular components of reflection into an image without specular highlights and an image of just the specular highlights.

The work of [Gershon, Jepson and Tsotsos 1987] exploits the color shifting that takes place on specular highlights on dielectrics towards the color of the illuminant. This is used to detect specular highlights rather than to quantitatively separate diffuse and specular components. Both this technique and the previously mentioned technique would not work if the illuminator were the same color as the object.

The technique presented in this paper presents a new approach to the quantitative separation of diffuse and specular components of reflection on object surfaces. This approach is based on the polarization, rather than the spectral (i.e. color) properties of reflected light. The polarization state of light differs on specular highlights than on regions which have just diffuse reflection. This is due to the fact that the polarization state of the diffuse component is different from that of the specular component. This property is seen to have advantages over spectrally based techniques because it is universal to both metals and dielectrics and holds regardless of object or illumination color.

The polarization state of reflected light is measured by using a linear polarizer, such as a Polaroid filter, placed in front of the imaging device. Taking two images with the polarizer oriented in two respective linearly independent orientations resolves the two polarization components of reflected light in these directions. At each pixel the two polarization components form a coordinate pair in 2-dimensional *polarization space*. The set of polarization coordinate pairs for pixels corresponding to an object made of a homogeneous material, form a linear cluster in polarization space. This linear cluster is predicted by the theory for how materials polarize light presented in [Wolff 1987].

[2] The body component of reflection is produced by light rays that penetrate into the surface of the object and then back out. The reason why the Dichromatic Reflection Model does not hold for metals is because they do not possess a body component of reflection.

[3] The interface component of reflection is produced by light rays that singularly or multiply reflect off of microfacets.

If the linearly independent components of polarization are taken parallel and perpendicular with respect to the plane in which specular rays travel [4] it will be shown that the slope of the line represented by a linear cluster in polarization space can be used to resolve the magnitudes of the diffuse and specular reflection components. The experimental results presented below resolve diffuse and specular reflection components using only a single light source. For extended lighting, more than two images need be taken for different orientations of the polarizer in front of the camera. This will be presented at a future date.

A number of examples of separation of reflection components on dielectrics and metals will be shown including images which contain both a dielectric and a metal. The set of polarization coordinates for pixels which correspond to an inhomogeneous material will be shown to form a wide linear cluster in polarization space. Objects in the same image which are made up of different materials altogether produce polarization coordinate pairs that produce different linear clusters. Materials forming linear clusters which are simple translations of each other are essentially the same except they have different albedo. Materials forming linear clusters having different slopes have different indices of refraction. As a consequence of the results of [Wolff 1988] pixels that produce polarization coordinate pairs that lie on linear clusters with slope greater than 3 most probably correspond to dielectric material while if they lie on linear clusters with slope between 1.0 and 2.0 they most probably correspond to metallic material.

The techniques presented here do not require any knowledge of the imaging geometry and are independent of the orientation of the object surface. It is recommended that the phase angle (i.e. the angle between the incident light source orientation and the viewing orientation) be above 90 degrees for best results with respect to camera noise, but in the presence of low noise levels, any phase angle will work. The techniques presented here for separating diffuse and specular components of reflection will be shown to work for surfaces that are polished as well as surfaces which have a rough level of detail. Experimentation with coated surfaces will be performed at a future date.

2 REFLECTION AND POLARIZATION OF LIGHT FROM OBJECT SURFACES

Material surfaces are assumed to have a microscopic level of detail which consists of a statistically large distribution of specularly reflecting planar microfacets. Each planar microfacet is perfectly smooth. Most light that is reflected from a material surface arises from the following three phenomena:

- Light rays which specularly reflect off a planar microfacet a single time.
- Light rays which go through at least two multiple specular reflections amongst multiple planar microfacets.
- Light rays which penetrate into the top layer of the material surface and then are reflected back out.

These three phenomena are illustrated in figure 1.

In the Dichromatic Reflection Model, the body component of reflection consists of the third phenomenon, while the interface component consists of the first two phenomena. In this paper the *diffuse component* of

[4] This plane is called the *specular plane of incidence* and is determined by the light source orientation vector and the viewing vector.

reflection will at least consist of the second and the third reflection phenomena. In addition to a microscopic planar microfacet level of detail, some rough materials can also have a rough level of detail that is visible but yet smaller than a pixel projected out onto the object. This is true for brushed metal surfaces. Multiple reflections amongst this level of surface detail is considered to contribute to the diffuse component. Also protrusions from other regions of a surface material can contribute to the diffuse component of reflection at a point in the form of stray light reflections. The *specular component* will consist of only the first reflection phenomenon listed above.

For both metals and dielectrics the diffuse component of reflection arises from multiple random reflection processes. Because of this, the polarization of the diffuse component of reflection is assumed to be always nearly completely unpolarized. This is especially true when the reflected light was initially unpolarized (before reflection) which is true for most common light sources.

The polarization of the specular component of reflection is dictated by the *Fresnel reflection coefficients*, for the material surface. The Fresnel reflection coefficients, $F_\perp$ and $F_\parallel$ vary between 0 and 1 inclusive and represent the proportional attenuation of the perpendicular and parallel components of a light ray that is specularly reflected once. The Fresnel reflection coefficients only depend upon the specular angle of incidence, Ψ', and the (complex) index of refraction $\eta = n - \kappa i$ which is dependent on material properties. The coefficient of extinction, κ, is zero for dielectrics in which case η is real. In terms of Ψ' and η, the Fresnel reflection coefficients are given by the following equations [Siegel and Howell 1981]:

$$F_\perp(\Psi', \eta) = \frac{a^2 + b^2 - 2a\cos\Psi' + \cos^2\Psi'}{a^2 + b^2 + 2a\cos\Psi' + \cos^2\Psi'}$$

$$F_\parallel(\Psi', \eta) = \frac{a^2 + b^2 - 2a\sin\Psi'\tan\Psi' + \sin^2\Psi'\tan^2\Psi'}{a^2 + b^2 + 2a\sin\Psi'\tan\Psi' + \sin^2\Psi'\tan^2\Psi'} F_\perp(\Psi', \eta)$$

where

$$2a^2 = [(n^2 - \kappa^2 - \sin^2\Psi')^2]^{1/2} + n^2 - \kappa^2 - \sin^2\Psi'$$

$$2b^2 = [(n^2 - \kappa^2 - \sin^2\Psi')^2]^{1/2} - (n^2 - \kappa^2 - \sin^2\Psi') \,.$$

The value for $F_\perp$ is always greater than or equal to $F_\parallel$ for all specular angles of incidence ranging from 0^0 to 90^0. Hence for initially unpolarized light, the polarization of the specular component of reflection is biased toward the normal to the specular plane of incidence. That is the perpendicular component of polarization of the specular component is larger than the parallel component. The ratio of the magnitude of the perpendicular polarization component to the parallel component for specular reflection is given by $F_\perp / F_\parallel$. Since the total reflected light from a point on an object surface also includes a diffuse component, the total perpendicular component and total parallel component will be made more equal because the diffuse component is unpolarized. As a consequence of the polarization theory in [Wolff 1987] the equations for the total perpendicular component, $k_\perp$, and total parallel component, $k_\parallel$ respectively are given by

$$\begin{aligned} (1/2)I_d + [\tfrac{F_\perp}{F_\parallel + F_\perp}]I_s &= k_\perp \\ (1/2)I_d + [\tfrac{F_\parallel}{F_\parallel + F_\perp}]I_s &= k_\parallel \end{aligned} \qquad (1)$$

where I_d and I_s are the magnitudes of the diffuse and specular reflection components respectively. The values for $k_\perp$ and $k_\parallel$ are measured by a camera with a polarizer oriented perpendicular and parallel respectively to the specular plane of incidence. The idea is to solve for I_d and I_s.

At first equations 1 appear to involve two equations in four unknowns, $F_\perp$, $F_\parallel$, I_d, and I_s. The number of variables can be reduced by defining the *Fresnel ratio* $q = F_\perp/F_\parallel$ and equivalently expressing equations 1 as

$$\begin{aligned} (1/2)I_d + [\tfrac{q}{1+q}]I_s &= k_\perp \\ (1/2)I_d + [\tfrac{1}{1+q}]I_s &= k_\parallel . \end{aligned} \tag{2}$$

Subtracting $(1/2)I_d$ from both equations in equations 2 and then dividing the first equation by the second gives

$$q = \frac{k_\perp - (1/2)I_d}{k_\parallel - (1/2)I_d} . \tag{3}$$

The following two sections explain different methods for computing q using equation 3. It is shown that accurate knowledge of the Fresnel ratio q leads to good segmentations of specular highlights and good quantitative separation of diffuse and specular components of reflection.

3 A FIRST ATTEMPT AT SEGMENTING SPECULAR HIGHLIGHTS

The computation of $q = F_\perp/F_\parallel$ in [Wolff 1988] is performed at specular highlights where the magnitude of the diffuse component, I_d, is relatively small compared to the specular component. Judging from equation 3, if both $k_\perp$ and $k_\parallel$ are composed of much of the specular component, they will both dominate the value of $(1/2)I_d$. Therefore a good approximation to q is made by the ratio of the perpendicular polarization component to the parallel polarization component, $k_\perp/k_\parallel$. From simple arithmetic, this ratio will always underestimate the true value of the Fresnel ratio, q. Unfortunately this value for q cannot be substituted back into equations 2 to solve for I_d and I_s since it is automatically implied from the approximate derivation of q that $I_d = 0$. However, again from equations 2, values of $k_\perp/k_\parallel$ that are larger than 1.0 imply the existence of a non-zero specular component. Of course this assumes that the specular angle of incidence is such that $F_\perp$ and $F_\parallel$ are not equal which is true for all angles except 0^0 and 90^0 which are not practical anyway. Therefore, theoretically speaking, the way to detect points on an object surface with a non-zero specular component of reflection is to threshold at 1.0 the ratio image created by the perpendicular and parallel components of polarization.

Unfortunately thresholding a ratio image at 1.0 is not practical since there is inherent noise to the gray level values of pixels. If the gray value of a particular pixel is observed for exactly the same scene over many images, the recorded gray values will vary over a distribution whose non-zero standard deviation, σ, is usually defined to be the *repeatability*. Therefore, a point on an object can be a perfectly diffuse reflecting region with $k_\perp = k_\parallel$, but the corresponding experimental gray values for the perpendicular and parallel component images could easily not be equal. Also, just because there may truly exist a non-zero specular component of reflection does not imply necessarily a point on a specular highlight region. Visually, a specular highlight occurs at points where the specular component of reflection is large enough to obscure object surface detail.

It may not be desirable to label "soft glossy highlight" regions in a binary image because segmenting these regions may obscure the segmentation of "hard glaring highlight" regions.

The segmenting of specular highlight regions on dielectric object surfaces can be adequately obtained from the thresholding of the ratio image of $k_\perp/k_\parallel$ at each pixel, using a specified constraint on the phase angle. It was discovered in [Wolff 1988] that, for dielectrics, the value for the Fresnel ratio $q = F_\perp/F_\parallel$ is at least 3.0 in the range of specular angles of incidence from 45^0 to 65^0 (phase angles from 90^0 to 130^0). Since the ratio $k_\perp/k_\parallel$ always underestimates the value of q, thresholding the polarization ratio image at 3.0 will detect points at which the specular component of reflection is very significant compared to the diffuse component of reflection. An example of this is shown in figure 2a for an orange ceramic cup with a white piece of paper taped onto the surface. Figure 2b shows the thresholded polarization ratio image at 3.0 . This image identifies specular highlight regions on the body and on the handle of the cup. Figure 2b could not be arrived at by simply applying an intensity threshold to figure 2a because the high albedo on the white paper makes some pixel values in this region higher than for pixels on the specular highlight on the handle.

The threshold for polarization ratio images of 3.0 and the constraint on the phase angle is very conservative. Note that even though there is a constraint on the phase angle, it is not required that the value of the phase angle be actually known. A threshold for polarization ratio images (for dielectrics) of 2.0 with a phase angle constraint between 70^0 and 150^0 produces very good results with some of the "softer highlights" flushed out a little.

Segmenting specular highlights on metals using the thresholding of polarization ratio images is a bit harder than for dielectrics, mostly due to the problem of image sensor noise. The polarization of specular highlights on metals are not as nearly biased towards the normal to the specular plane of incidence as for dielectrics. This means that the ratio $k_\perp/k_\parallel$ is much closer to 1.0, even in cases of very harsh highlights. It was determined both theoretically and empirically in [Wolff 1988] that the true Fresnel ratio for metals rarely goes higher than 2.0 and can get very close to 1.0 for some metals at most phase angles.

Specular highlights on polished metal surfaces can get extremely bright which is a problem for CCD cameras whose intensity response curves are usually very flat (i.e. horizontal) at high incident radiance (e.g. gray value 240). With such a flat response curve, even small variations in gray value due to sensor repeatability can cause large variations in the interpretation of how much reflected radiance is incident on the camera. Therefore, experimental values for $k_\perp/k_\parallel$ can potentially get to be large (e.g. between 1.0 and 1.5) for points where in reality $k_\perp$ is identical to $k_\parallel$. This is clearly not a problem for the segmentation of specular highlights from dielectrics since a threshold of at least 2.0 is used.

Figure 3a shows an illuminated metal wrench and figure 3b shows the corresponding thresholded polarization ratio image, thresholded at 1.5 . Figure 3b does identify the major specular highlight regions with some regions which may be a result of "soft highlights" or image sensor noise.

4 SEPARATION OF DIFFUSE AND SPECULAR COMPONENTS OF REFLECTION

In the previous section specular highlight regions were labeled in a binary image. A more accurate way to segment specular highlights from object surfaces is to separate the diffuse and specular components of reflection. In this way the magnitude of the specular component can be analyzed on an absolute scale or relative to the magnitude of the diffuse component. The diffuse component of reflection also serves as a

restoration of the visible level of detail of the object surface in the absence of specular reflection.

To determine the magnitudes of the diffuse and specular components in equations 2 it is required that q be known accurately. In the previous section, q was approximated at each point corresponding to a pixel from the polarization ratio $k_\perp/k_\parallel$. However, approximating q in this way and then solving equations 2 pixel by pixel will always yield a zero diffuse component (see equation 3). Also, a single pixel based approximation to q is a very tenuous measurement in the presence of noise from the image sensor, and in the presence of a significant diffuse reflection component. An object point corresponding to a pixel may have a moderate specular component accompanied by a relatively significant diffuse component making $k_\perp/k_\parallel$ a rather inaccurate approximation of q. Consider also the inaccuracy of this approximation when the specular angle of incidence is almost equal to the Brewster angle for a dielectric where $k_\perp$ is many times larger than $(1/2)I_d$ and $k_\parallel$ is very close to $(1/2)I_d$.

All of these problems related to the accurate determination of q can be greatly ameliorated when equation 3 is viewed as an equation in *polarization space* with coordinate pairs $(k_\parallel, k_\perp)$ produced from many pixels. Equation 3 is equivalently

$$k_\perp = qk_\parallel + \frac{(1-q)}{2} I_d \tag{4}$$

which over a set of pixels corresponding to points on a single object surface will determine a linear cluster of points in polarization space. The slope of a linear approximation to these points is the value of q and the diffuse component of reflection at specular highlights is easily determined from the intercept at $k_\parallel = 0$ which is $((1-q)/2)I_d$. Linear clusters are formed from pixels corresponding to all points on the object surface including specular highlights, softer highlight regions and diffuse regions.

The prediction that polarization coordinate pairs for pixels corresponding to points on a homogeneous surface form a linear cluster is based upon the assumption that each pixel will have a nearly constant diffuse component I_d (see equation 4). This is in fact true to a very good approximation for pixels corresponding to strong specular regions (i.e. specular highlights). For a nonextended light source, specular highlights occur for a very narrow range of local surface orientations. The diffuse component of reflection, which is usually Lambertian, will vary very little in this narrow range. The local surface orientations will become more diversified for the set of pixels with less of a specular component, and this results in polarization coordinate pairs which form a wider linear cluster. Fortunately the cluster becomes too wide for a good linear approximation only well below the gray level threshold that is used to remove stray light from background points. All polarization clusters shown below consist of points that have a perpendicular polarization component corresponding to a gray level of at least 80 .

The gradual tapering of a polarization space cluster for a homogeneous material can be observed in figure 4b which corresponds to the image of a blue plastic jug in figure 4a . The linear cluster has a wide base of points at more diffuse points which occur at lower $k_\perp$ values, but tapers off at higher $k_\perp$ values which are near specular highlight regions. The slope of the linear cluster was determined to be $q = 13.2$, and then solving equations 2 pixel by pixel produced figures 4c and 4d for the diffuse and specular reflection components respectively.

Figure 5a shows the image of a flat piece of brushed Aluminum metal and figure 5b shows the corresponding linear cluster in polarization space, determined to have slope $q = 1.21$. Because the surface is flat, the cluster has a thin taper at lower $k_\perp$ values and becomes thicker at higher values due to the flattening of the image sensor response curve and therefore less refined quantization of incident radiance. Figures 5c and 5d show images of the diffuse and specular components of reflection respectively. Note how the elliptical

outline projections of both the circular light source and the outer surrounding lamp reflector can be made out far more clearly in the specular component image (figure 5d) than in the original image. The specular component image also reveals the reflection directly from the filament of the bulb as being the bright region near the northeast corner of the brushed Aluminum plate. The diffuse component image (figure 5c) possesses low gray values in the region where the bulb is reflecting off the surface. This implies the existence of very few multiple reflections in this region. The same for the circular dark band also in the diffuse component image. The brushed Aluminum plate contained additional scratches and smudge marks which account for some of the irregularities seen in the diffuse component image. Some points are black in both images which correspond to pixels which could not be processed because of limitations caused by the repeatability of the CCD camera used.

Figure 6a is an image of a metal wrench with a rubber handle. Observe the plot of the polarization coordinate pairs in figure 6d. One is of a nearly vertical thin linear cluster, and the other is a "fuzzy" almost diagonal linear cluster. The respective slopes of these linear clusters are 151.0 and 1.43 . The very thin quality to the linear cluster with slope 151.0 is attributed to a very smooth surface where significant specular reflection occurs for an usually narrow range of surface orientations. At a particular pixel, the solution of equations 2 uses the q of the linear cluster to which the associated polarization coordinate pair corresponds too. From the work presented in [Wolff 1988] it is clear that the cluster with $q = 151.0$ corresponds to the rubber dielectric handle, and the cluster with $q = 1.43$ corresponds to the metal body of the wrench. Hence in addition to separating diffuse and specular reflection components, the method of plotting polarization coordinate pairs can identify the material makeup corresponding to certain pixels.

The corresponding specular and diffuse component images are contained in figures 6b and 6c respectively. Note how the polished metal part of the wrench has very little diffuse component of reflection (figure 6c) due to the absence of internal body reflection. The specular and diffuse components were not separated well at the metal bolt that holds the wrench together. This is due to the metal bolt being different from the metal in the wrench itself. The linear cluster for the the isolated metal bolt is contained somewhere in the larger cluster of points in polarization space in figure 6d for the metal part of the wrench. This demonstrates some difficult pattern recognition problems for linear clusters.

Another example of difficulty discerning between two linear clusters in polarization space occurs for the image in figure 7a with the plot of polarization coordinate pairs in figure 7b. The image of figure 7a is of a gray ceramic cup with a square patch of blue on which there is a strong specular highlight that crosses between the gray and blue regions. The ceramic material on the cup is quite rough. It was originally hoped that the only difference between the gray and blue regions would be a difference in albedo, in which case two distinct lines of the same slope would arise a constant translation from one another. Instead not only are the slopes for the gray and blue regions different, but the regions themselves are not very homogeneous in material makeup as can be seen by the relatively wide linear cluster. A hand segmentation using $q = 50$ for the gray region and $q = 30$ for the blue region yielded the diffuse and specular reflection components in figures 7c and 7d respectively. It is remarkable how the visible detail has been restored going from figure 7a to figure 7c .

Finally, the polarization coordinate pair plot of the orange ceramic cup in figure 2a (again shown in figure 8a) is given in figure 8d with resulting $q = 10.0$ for the large linear cluster. The small cluster to the right of the large cluster is the base of the linear cluster for the white piece of paper taped onto the cup. A value of $q = 10.0$ was used for all pixels to solve for the diffuse and specular reflection components in figure 8b and 8c respectively. Note the very slight specular component of reflection on the piece of paper. The magnitude of the specular component on the paper is probably a bit wrong since not enough of its corresponding linear

cluster in polarization space is available to derive its corresponding true q value. That is, the q value for the paper is different than that for the ceramic cup, and not enough information is available to accurately determine q for the paper.

5 CONCLUSION

A powerful new method has been presented using a polarizing filter to separate diffuse and specular components of reflection from object surfaces. A number of experimental results were presented which demonstrates that this method works for dielectric and metal surfaces both polished and rough. An example of separating reflection components from different materials in the same image was demonstrated as well as an example of separating reflection components from a rough dielectric with varying albedo. No *a priori* knowledge was required for the imaging geometry or the orientation of the object surfaces. Also, no knowledge is required of the color or intensity of the light source being used. This suggests that this method of separating specular and diffuse reflection components is quite robust.

The method for separating diffuse and specular components of reflection relies on the fact that the polarization states for these two components are different. By separating out the parallel and perpendicular components of polarization for reflected light using a polarizing filter, a respective two dimensional plot of points is generated. Each point coordinate pair corresponds to the parallel and perpendicular polarization magnitude at a pixel, respectively. These plots of points form linear clusters, and the measured value of the slopes of respective approximating lines is crucial to determine the magnitude of the diffuse and specular component of reflection. Sometimes difficult pattern recognition problems arise when linear clusters, caused by different albedo or different material, are close together. It was seen that the slope of these linear clusters can be used to classify a material according to whether it is metal or dielectric.

Future work will entail further improvements in resolving linear clusters in polarization space that are close together. Research will also proceed in actually determining local surface normals from component reflection information.

ACKNOWLEDGMENTS

The author would like to thank his faculty advisor Terry Boult for reviewing this paper and giving helpful suggestions.

References

[Barrow and Tenenbaum 1978] Barrow, H.G., and Tenenbaum, J.M., *Recovering Intrinsic Scene Characteristics from Images*, in *Computer Vision Systems*, A.R. Hanson and E.M. Riseman, Eds., Academic Press, New York, 1978, pp.3-26.

[Cook and Torrance 1981] Cook, R.L., and Torrance, K.E., *A Reflectance Model For Computer Graphics*, SIGGRAPH 1981 Proceedings, Vol. 15 #3 pp.307-316, 1981.

[Gershon, Jepson and Tsotsos 1987] Gershon, R., Jepson, A.D. and Tsotsos, J.K., *Highlight Identification Using Chromatic Information*, Proceedings of the First International Conference on Computer Vision, pp. 161-171. 1987.

[Klinker, Shafer and Kanade 1987] Klinker, G.J., Shafer, S.A. and Kanade, T., *Using A Color Reflection Model to Separate Highlights From Object Color*, Proceedings of the First International Conference on Computer Vision, pp. 145-150, 1987.

[Shafer 1985] Shafer, S.A., *Using Color To Separate Reflection Components*, COLOR research and application, 10(4), pp.210-218, Winter 1985.

[Siegel and Howell 1981] Siegel, R. and Howell, J.R., *Thermal Radiation Heat Transfer*, McGraw-Hill, 1981.

[Torrance and Sparrow 1967] Torrance, K.E., and Sparrow, E.M., *Theory For Off-Specular Reflection From Roughened Surfaces*, Journal Of The Optical Society Of America, Vol. 57 #9 pp.1105-1114, September 1967.

[Wolff 1987] Wolff, L.B., *Surface Orientation From Polarization Images*, SPIE Cambridge 1987, Volume 850, Optics, Illumination, and Image Sensing For Machine Vision II, pp.110-121.

[Wolff 1988] Wolff, L.B., *Classification Of Material Surfaces From The Polarization of Specular Highlights*, SPIE Cambridge 1988, Optics, Illumination, and Image Sensing For Machine Vision III.

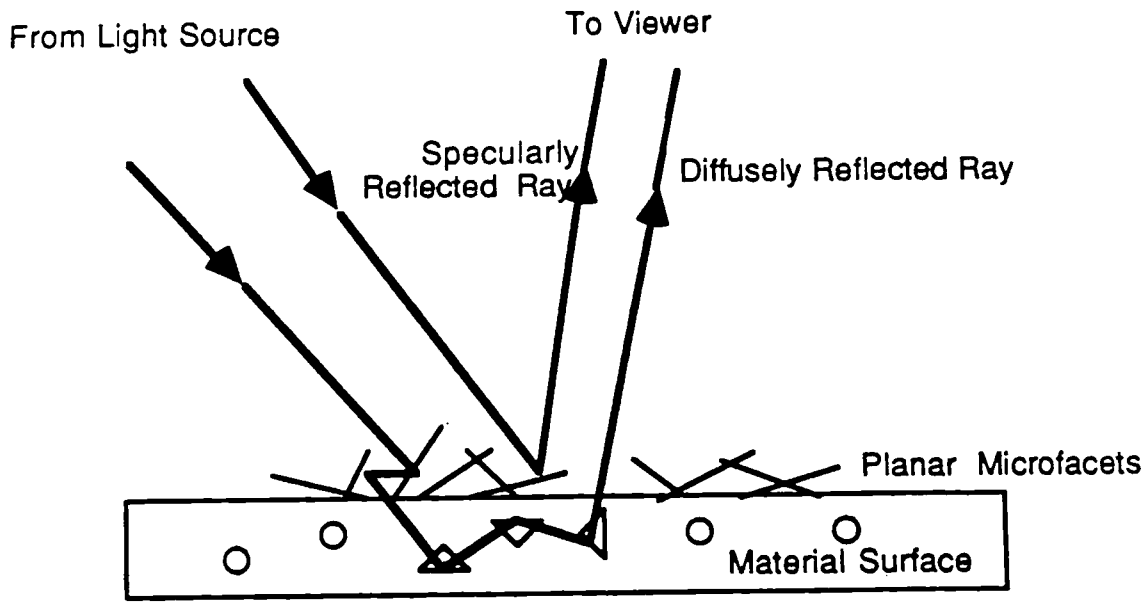
From Light Source
To Viewer
Specularly
Reflected Ray
Diffusely Reflected Ray
Planar Microfacets
Material Surface

FIGURE 1

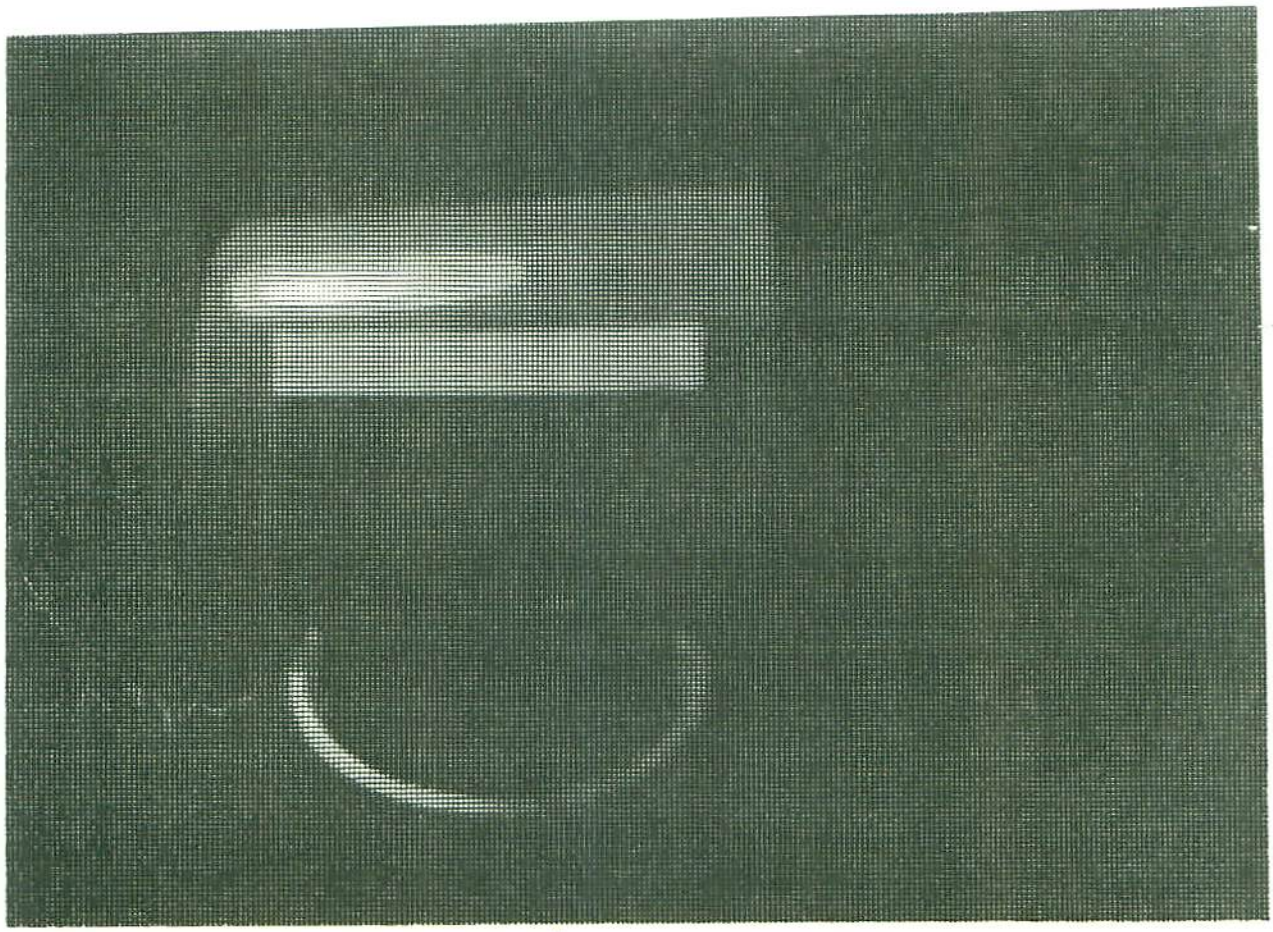

2(a)

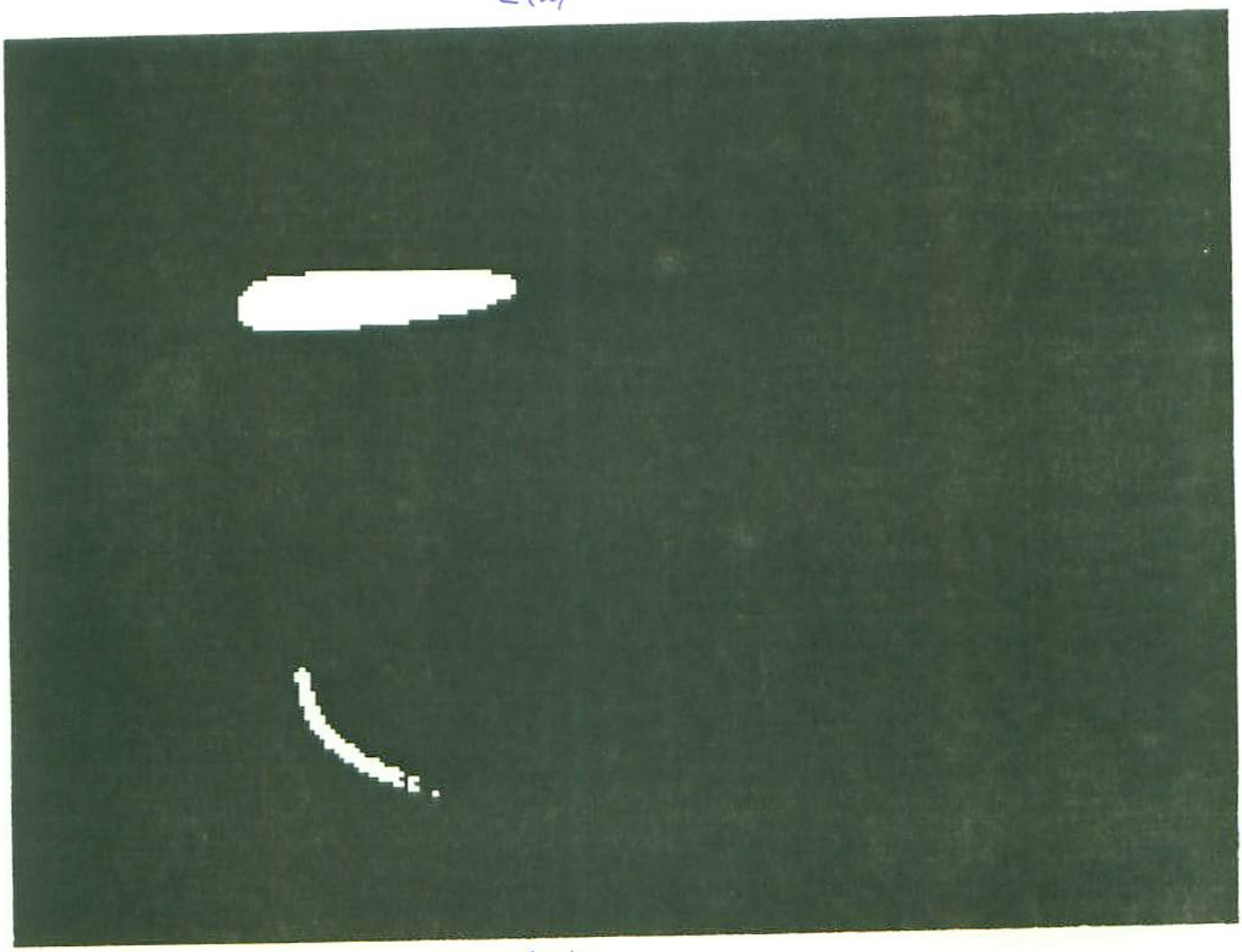

2(b)

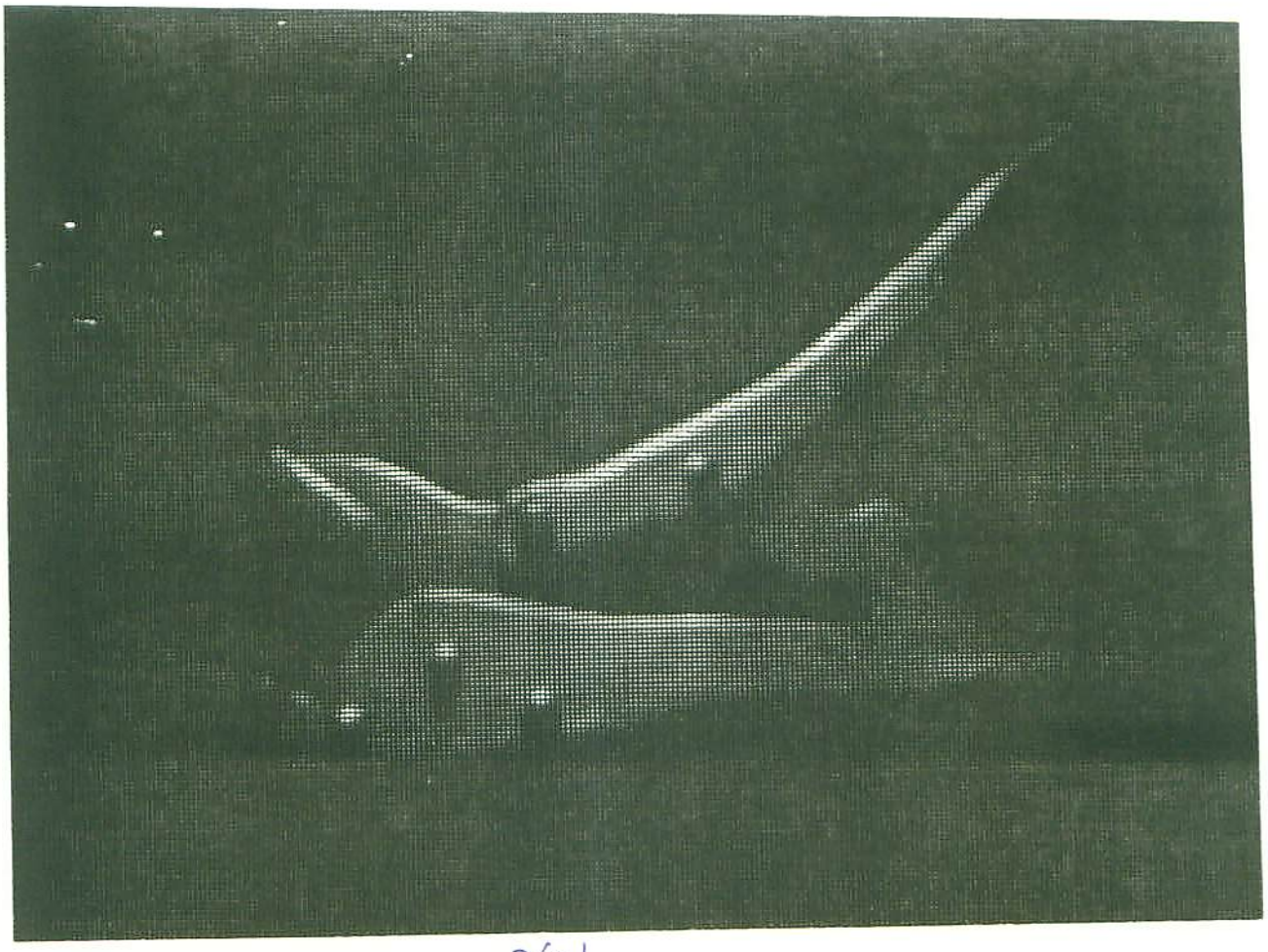

3(a)

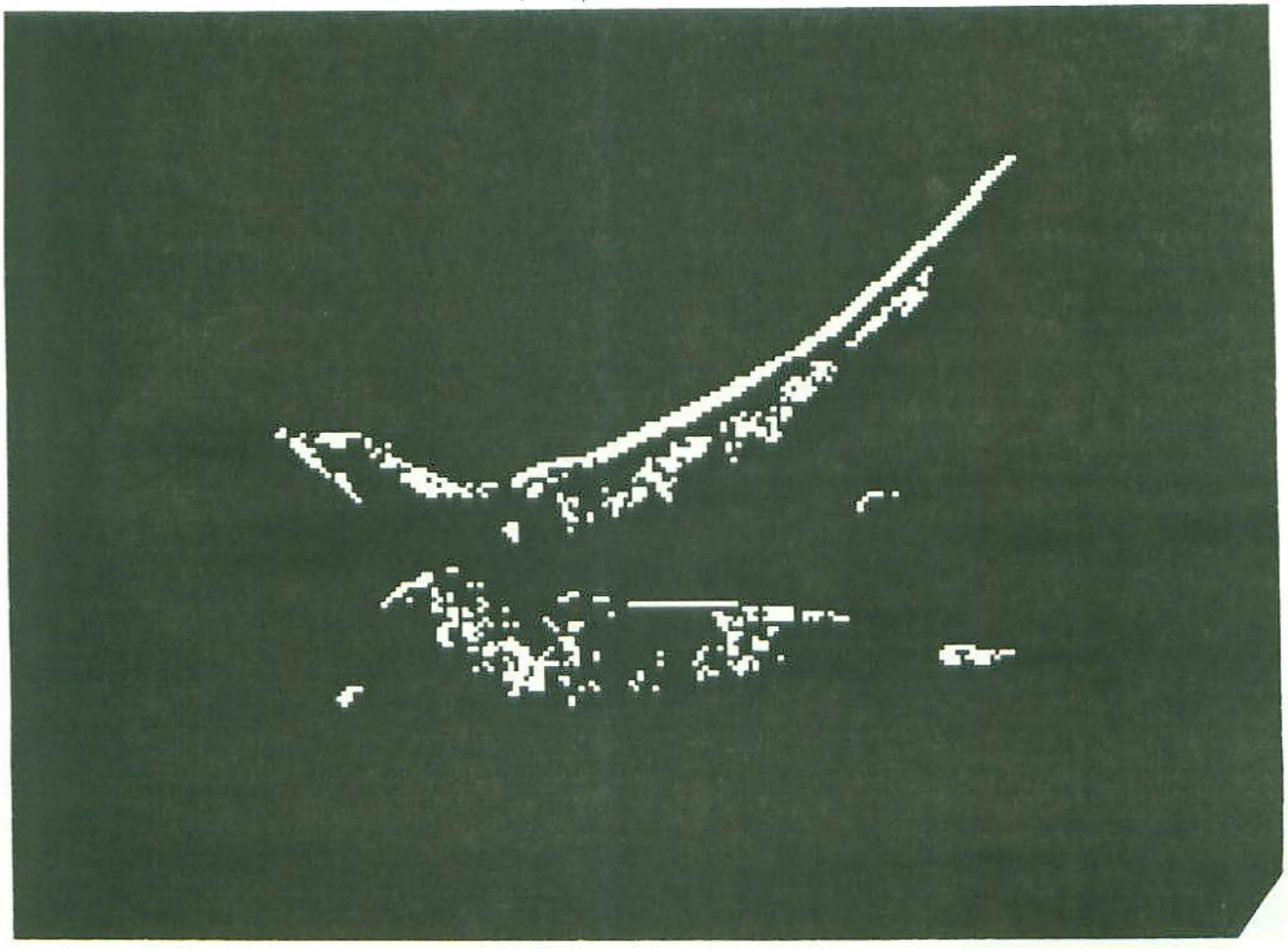

3(b)

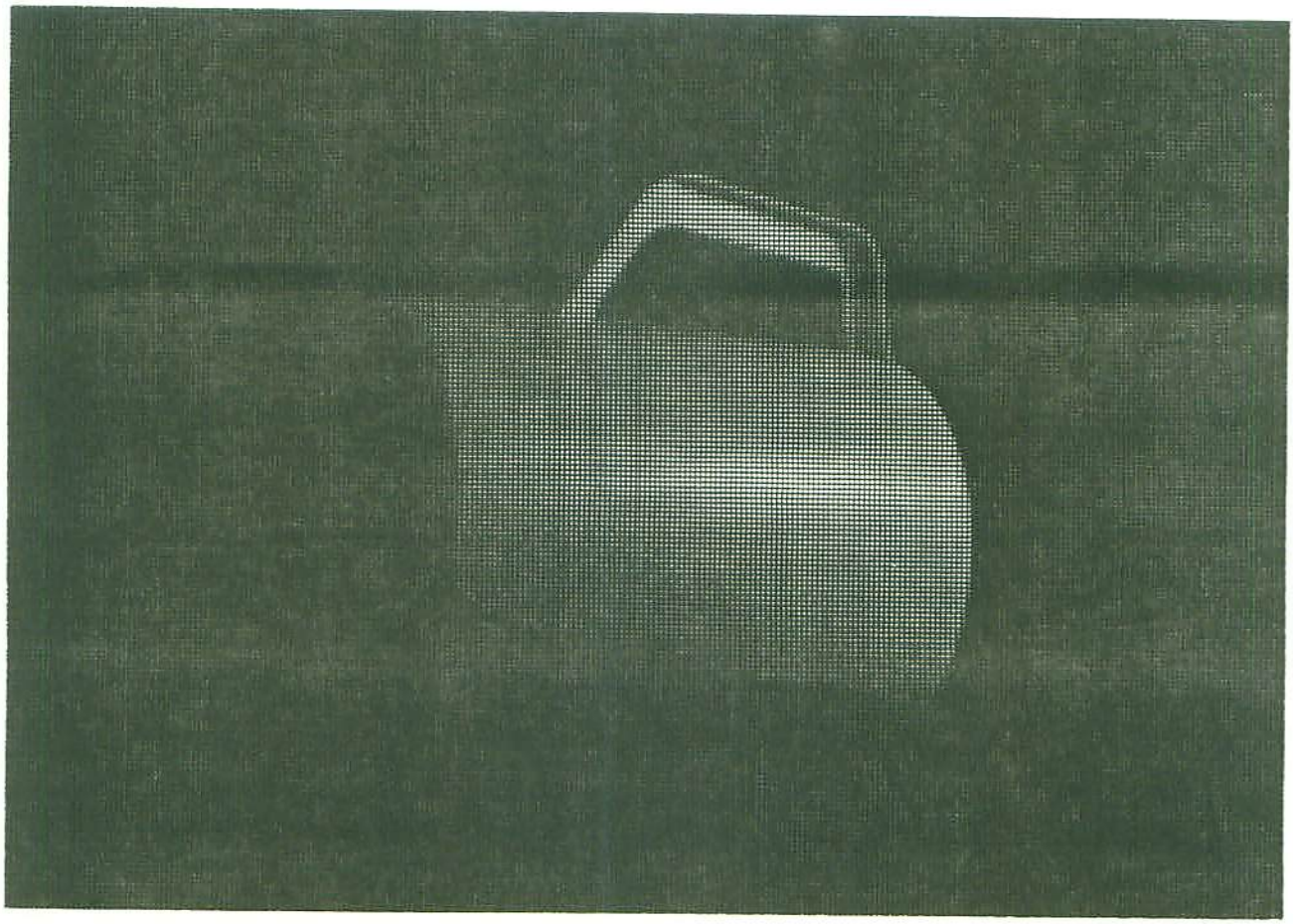

4(a)

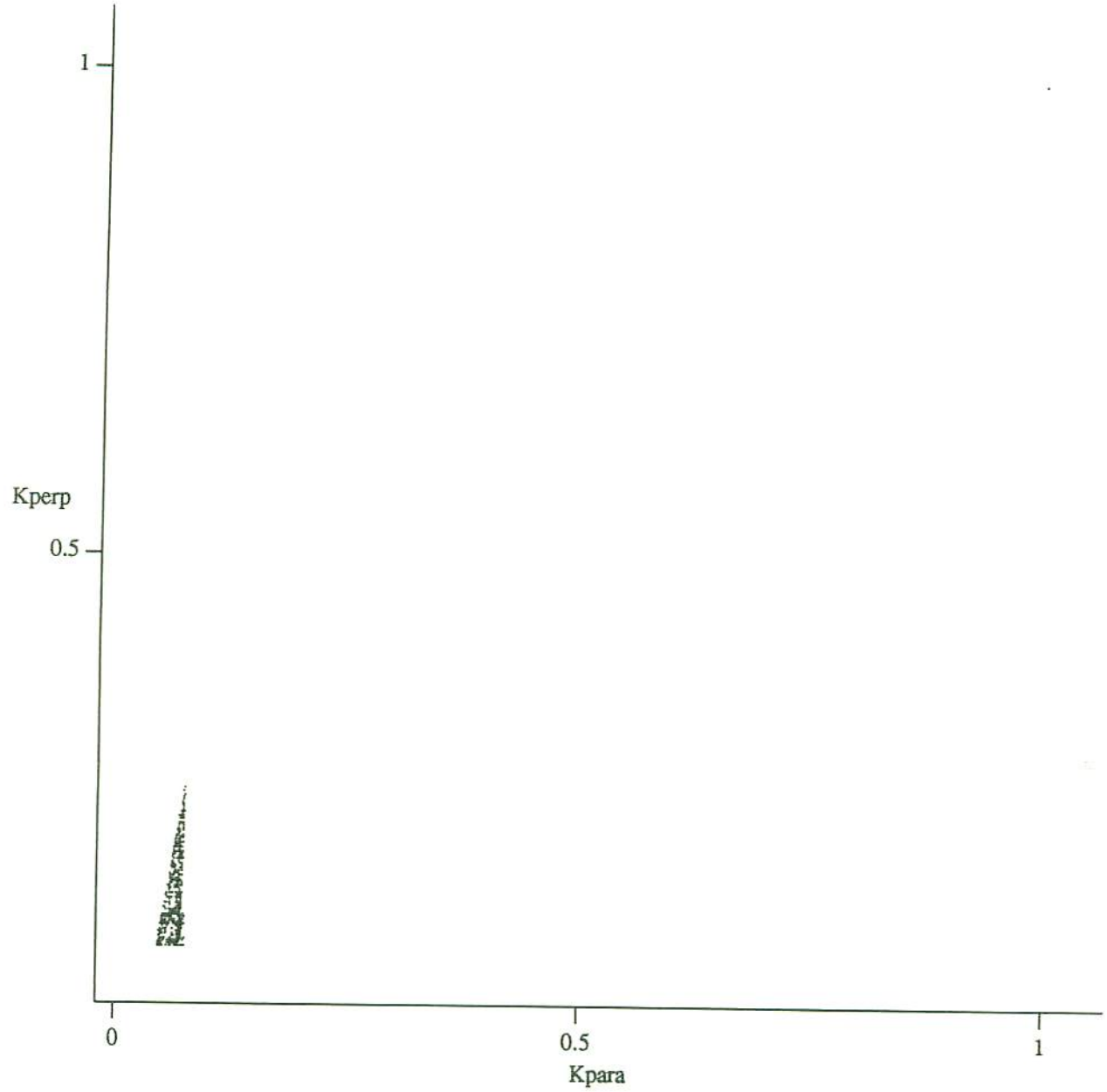

LINEARIZED Kperp vs Kpara FOR BLUE JUG

4(b)

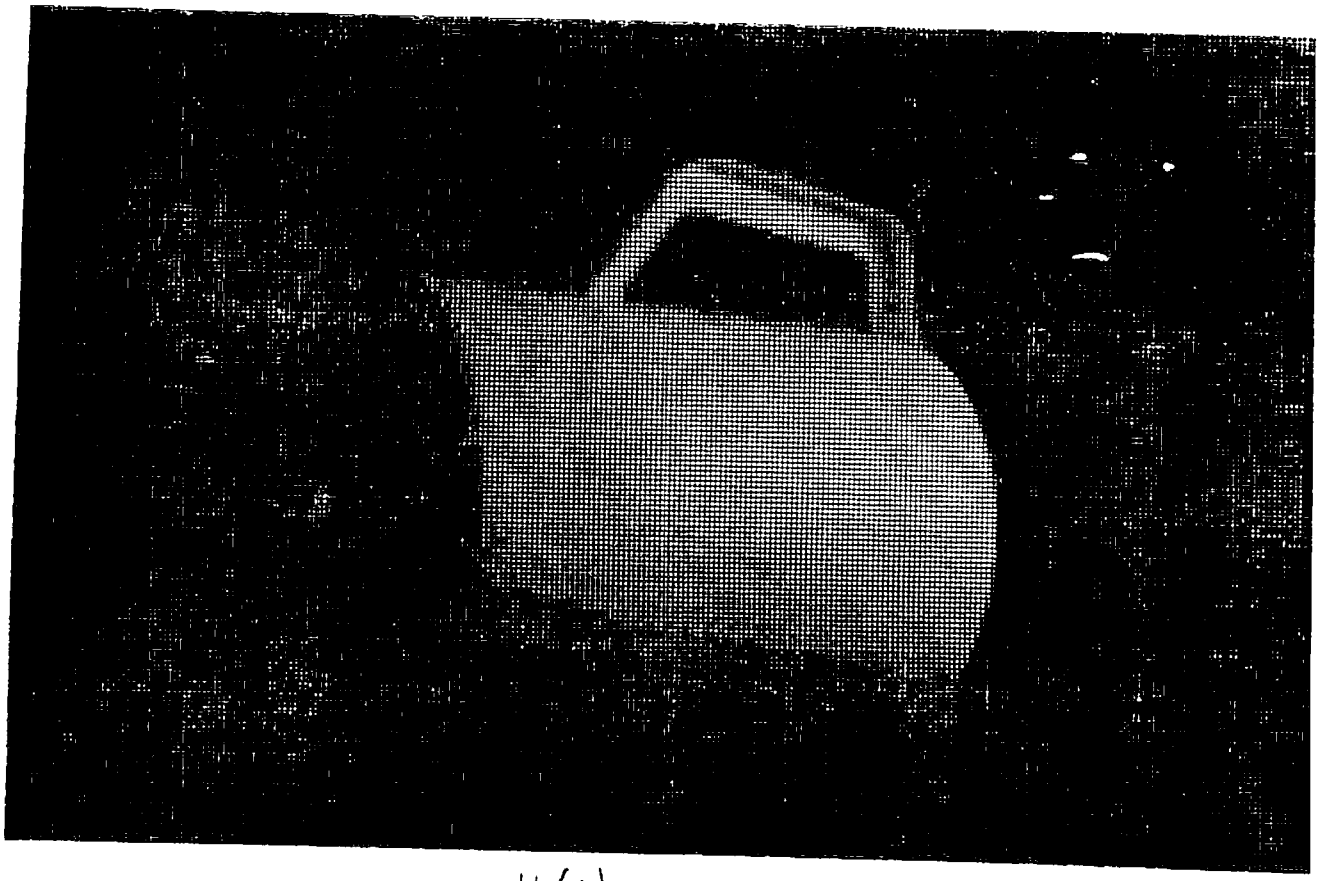

4(c)

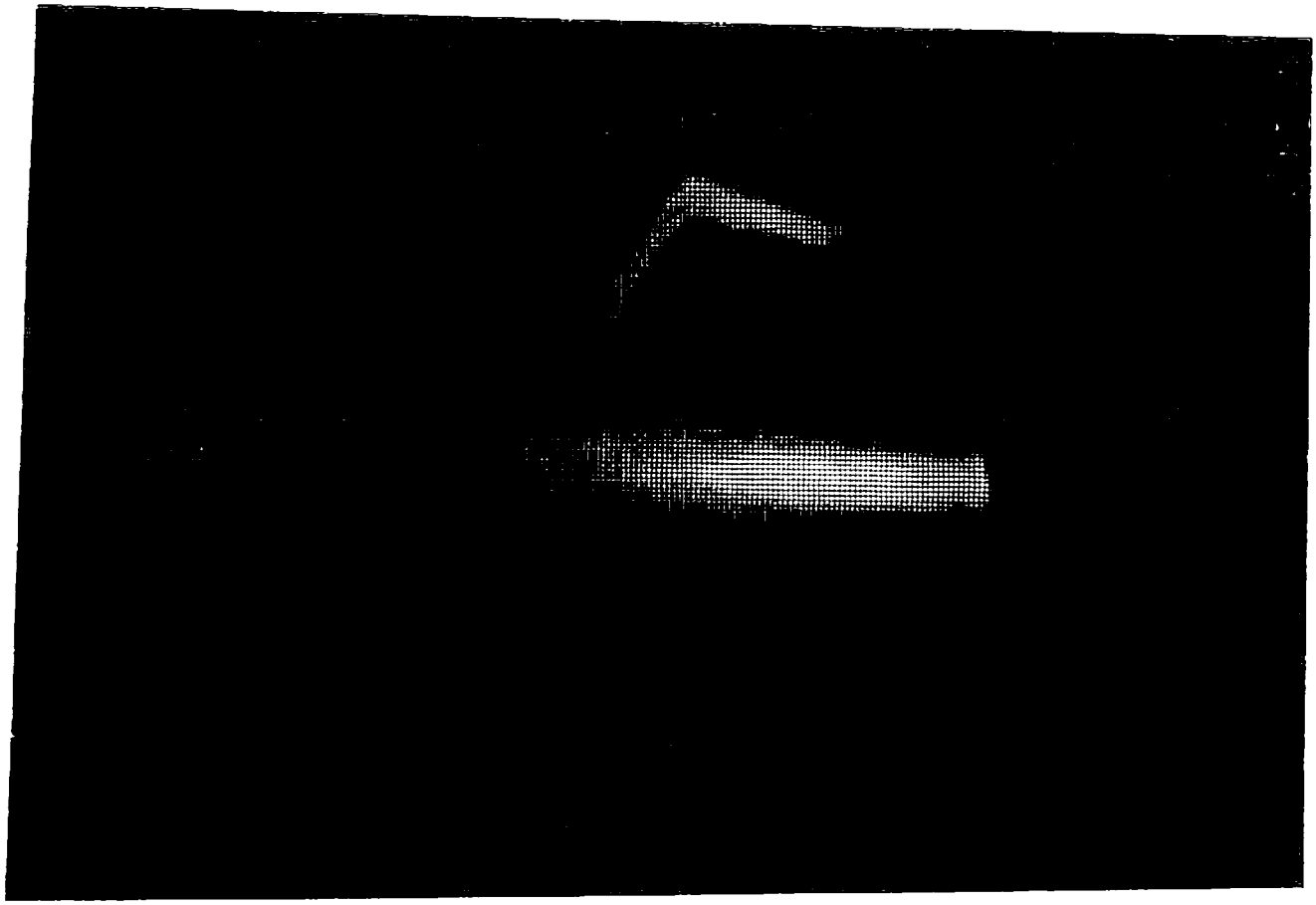

4(d)

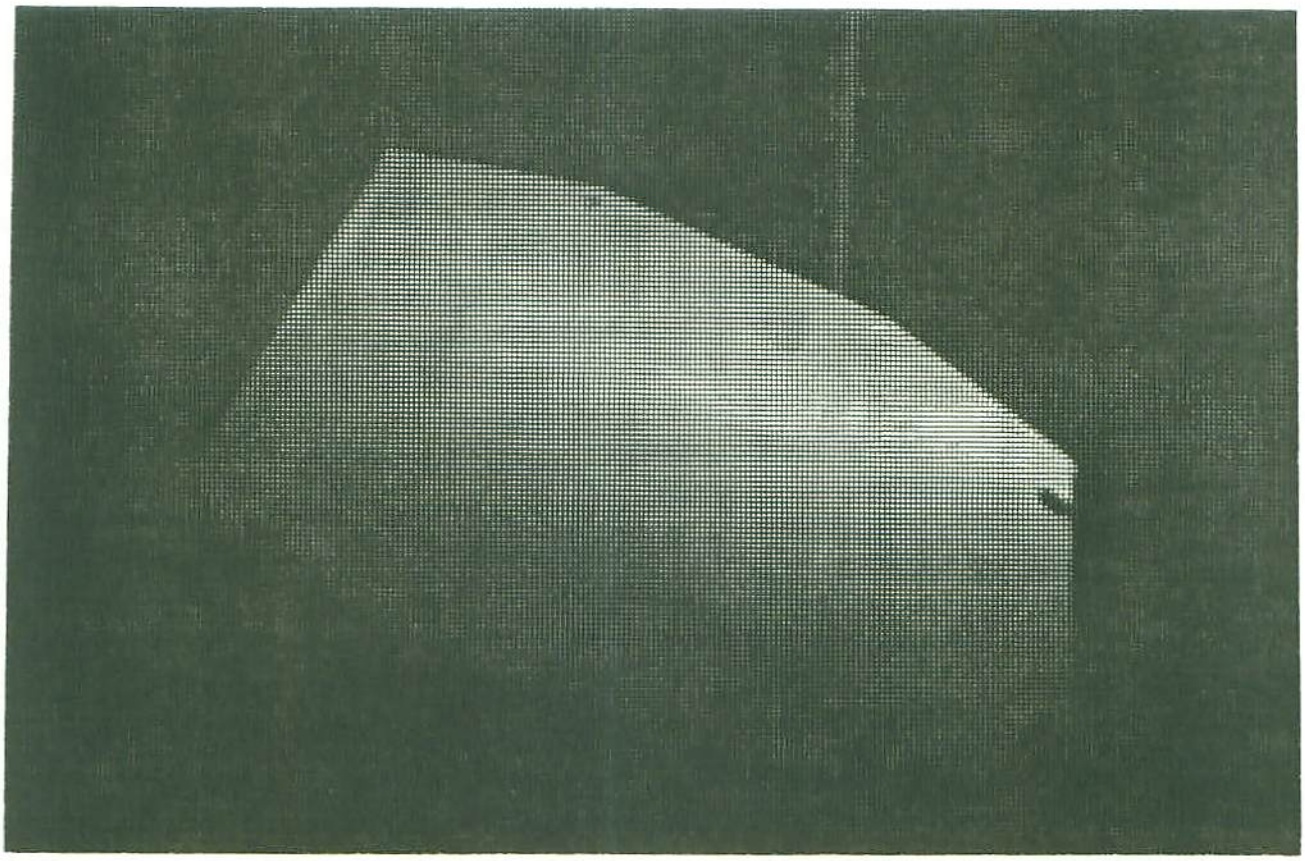

5(a)

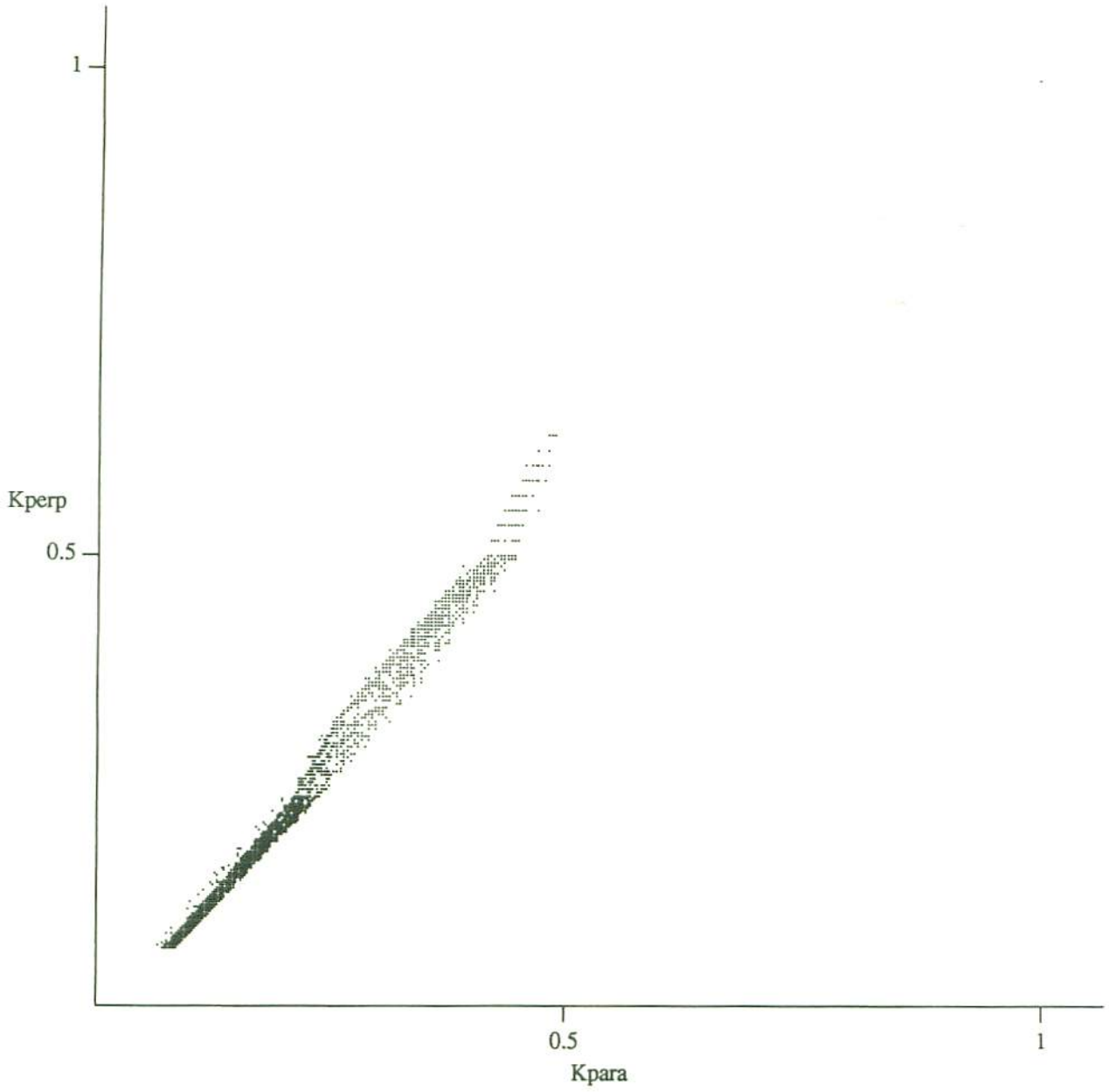

LINEARIZED Kperp vs Kpara FOR [redacted] BRUSHED ALUMINUM

5(b)

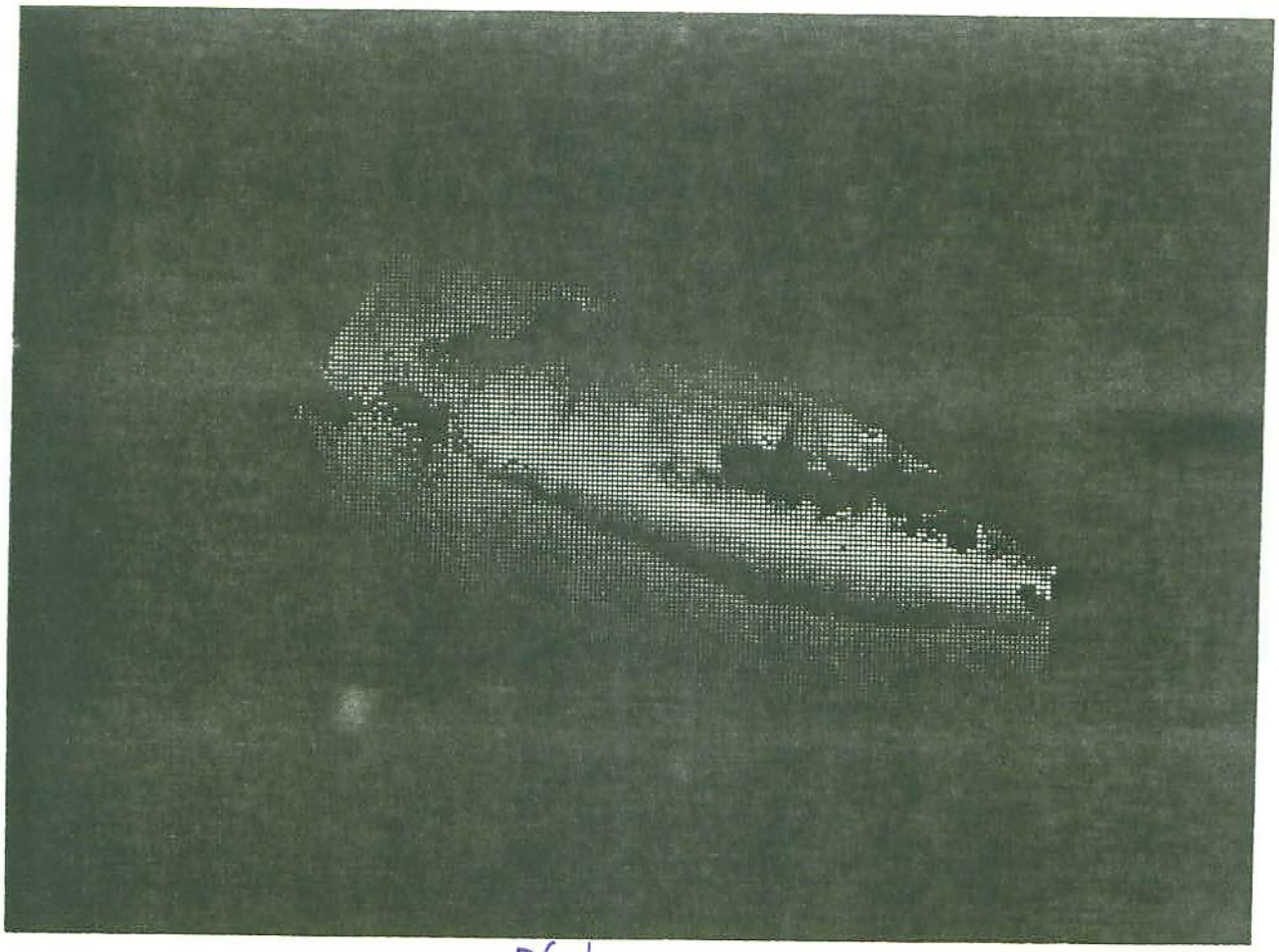

5(c)

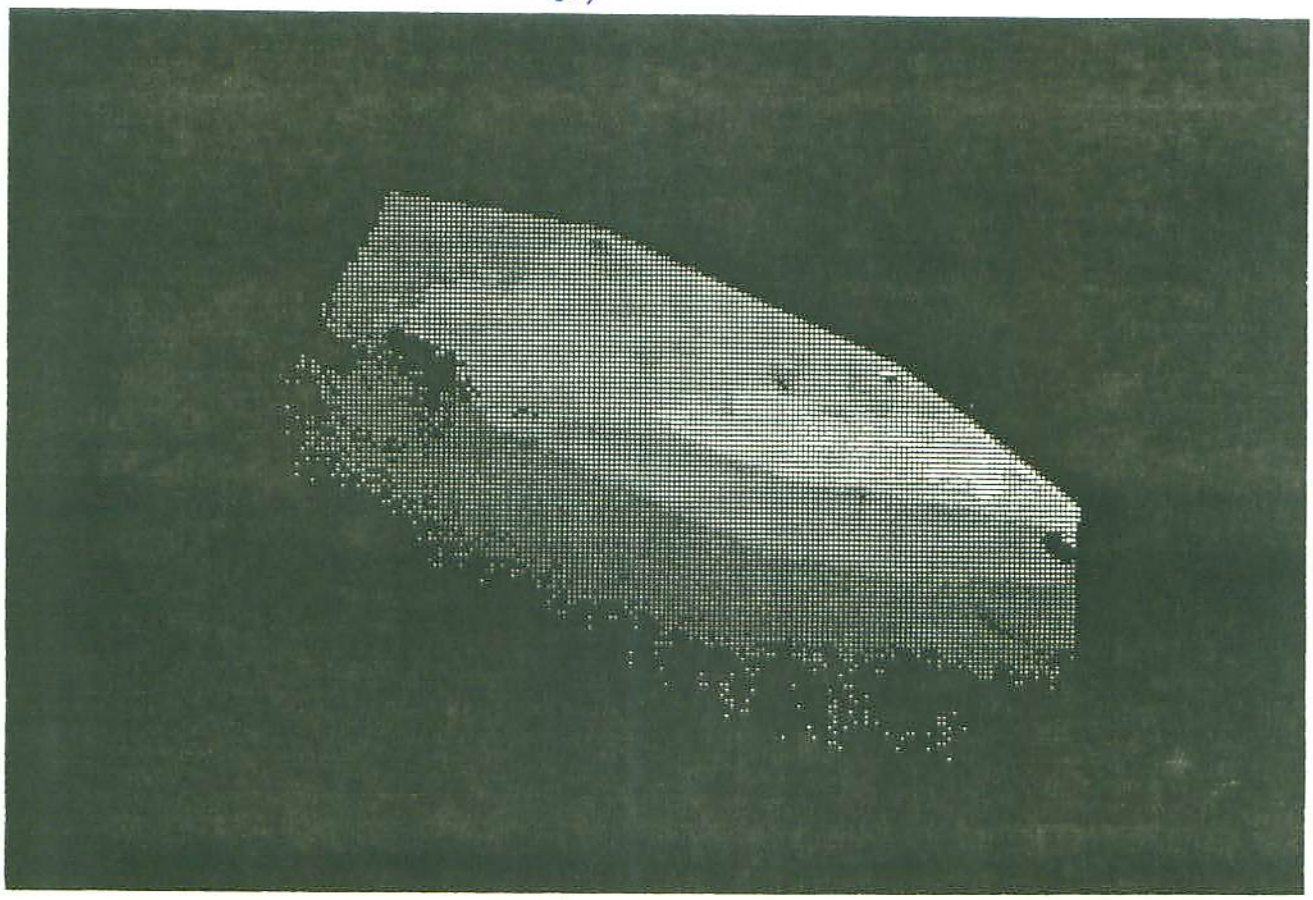

5(d)

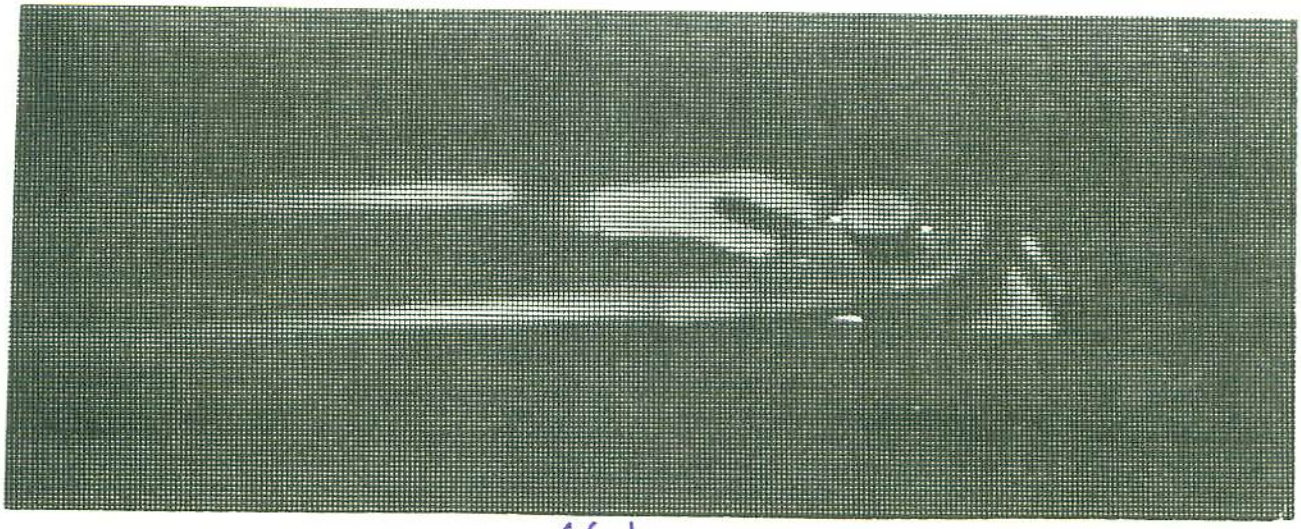

6(a)

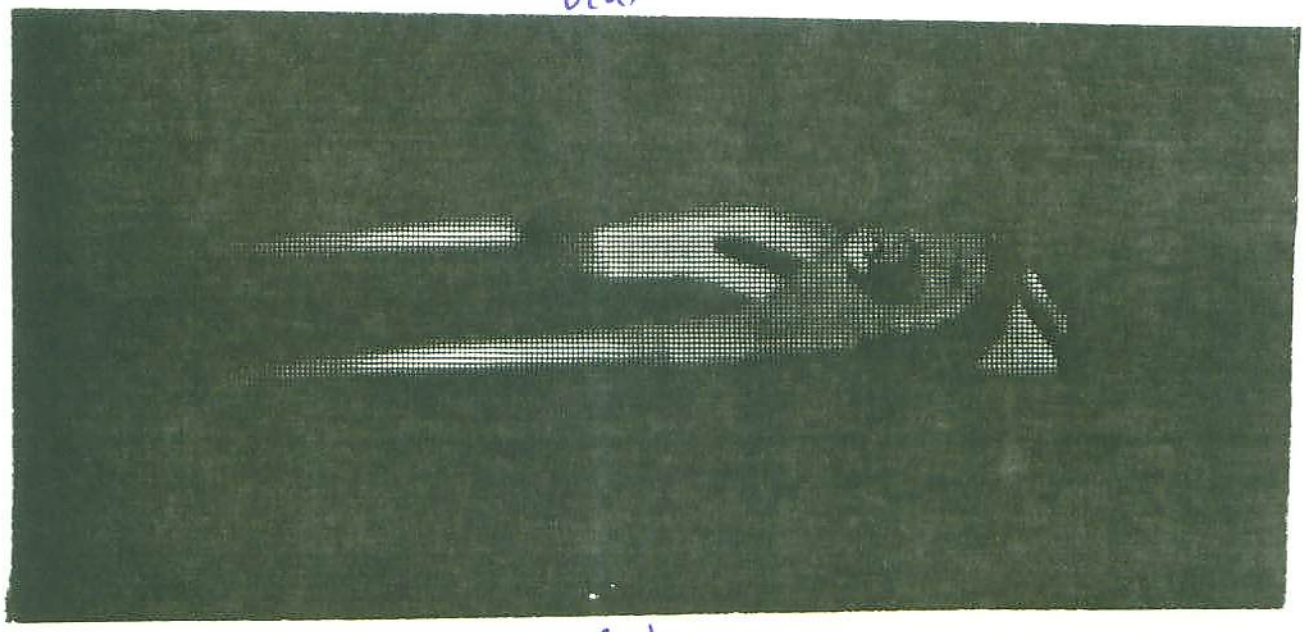

6(b)

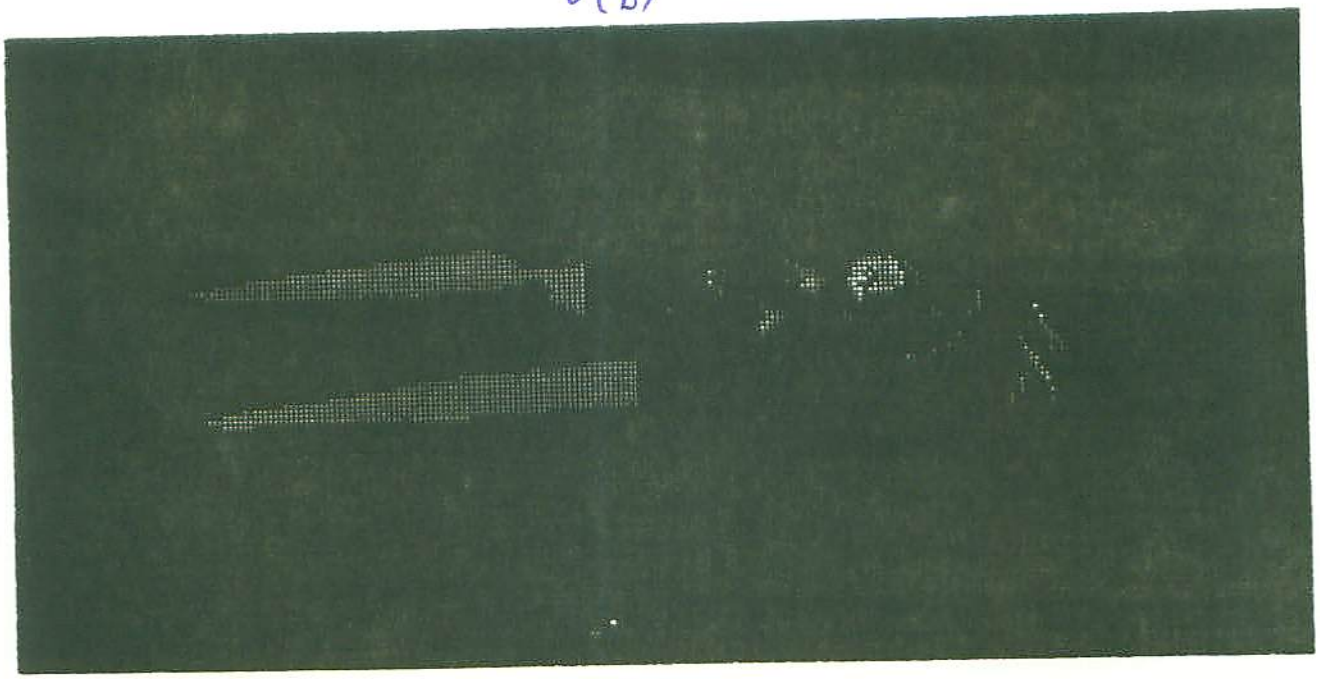

6(c)

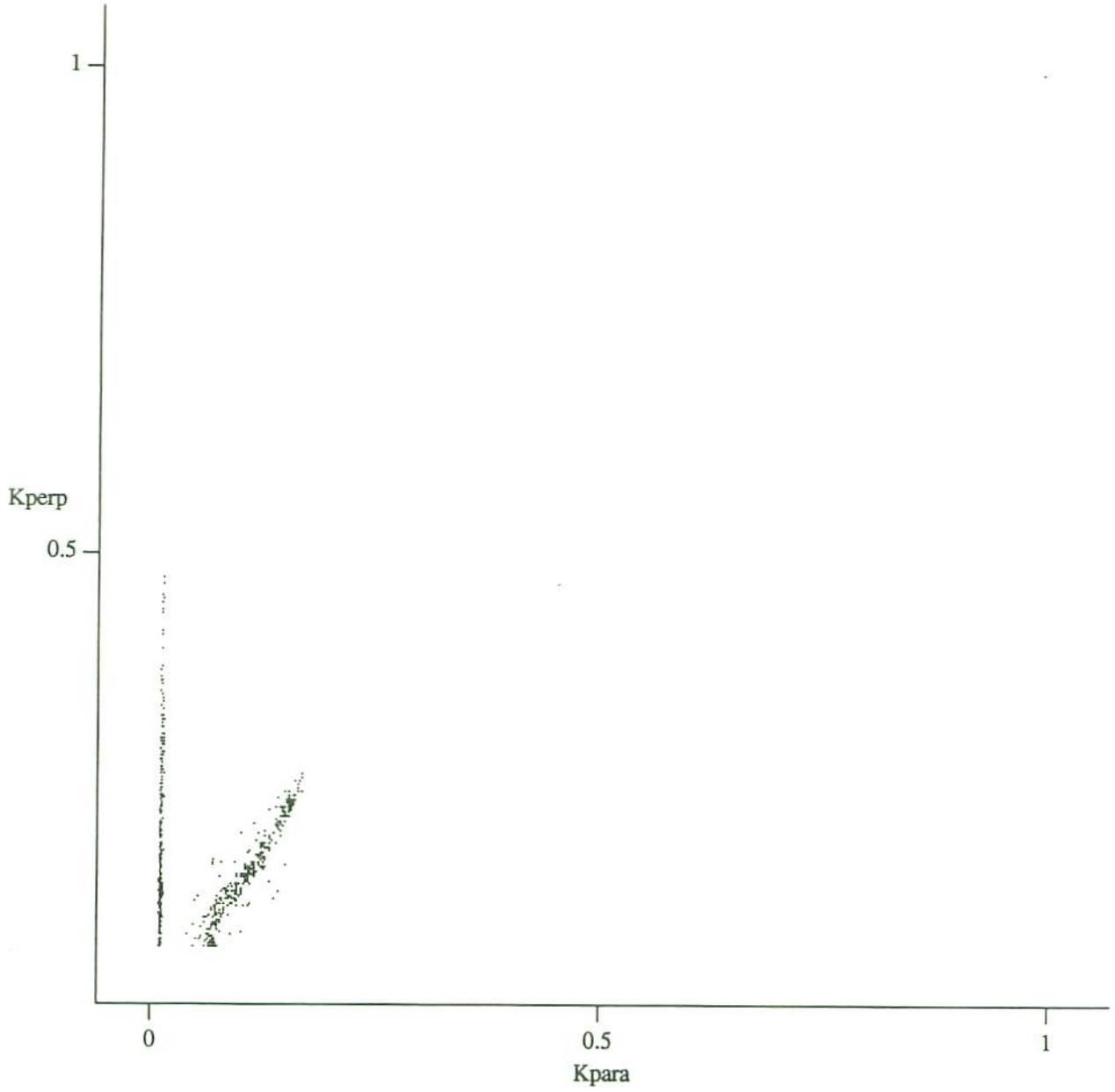

LINEARIZED Kperp vs Kpara FOR METAL WRENCH WITH RUBBER HANDLE

6(d)

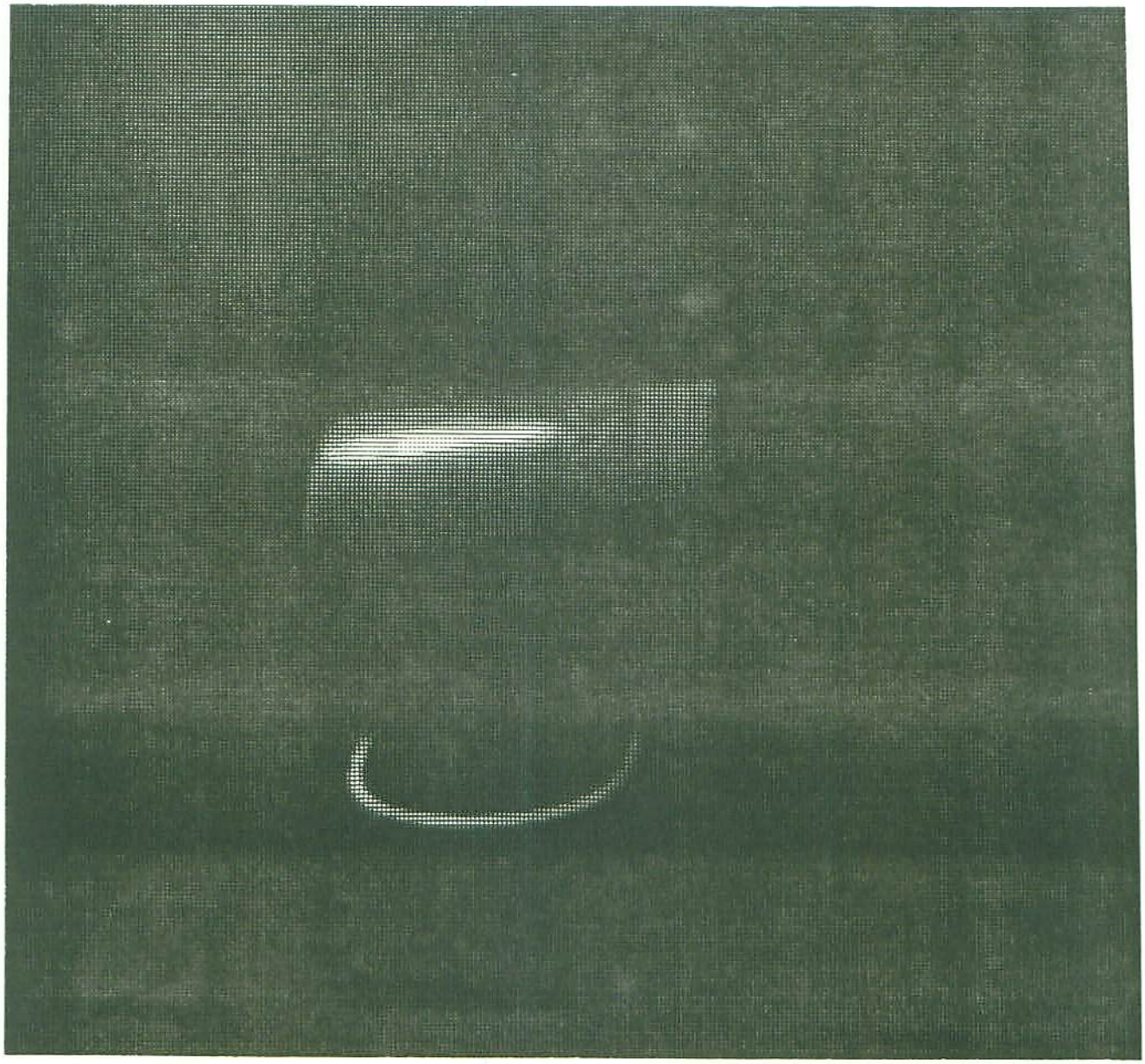

7(a)

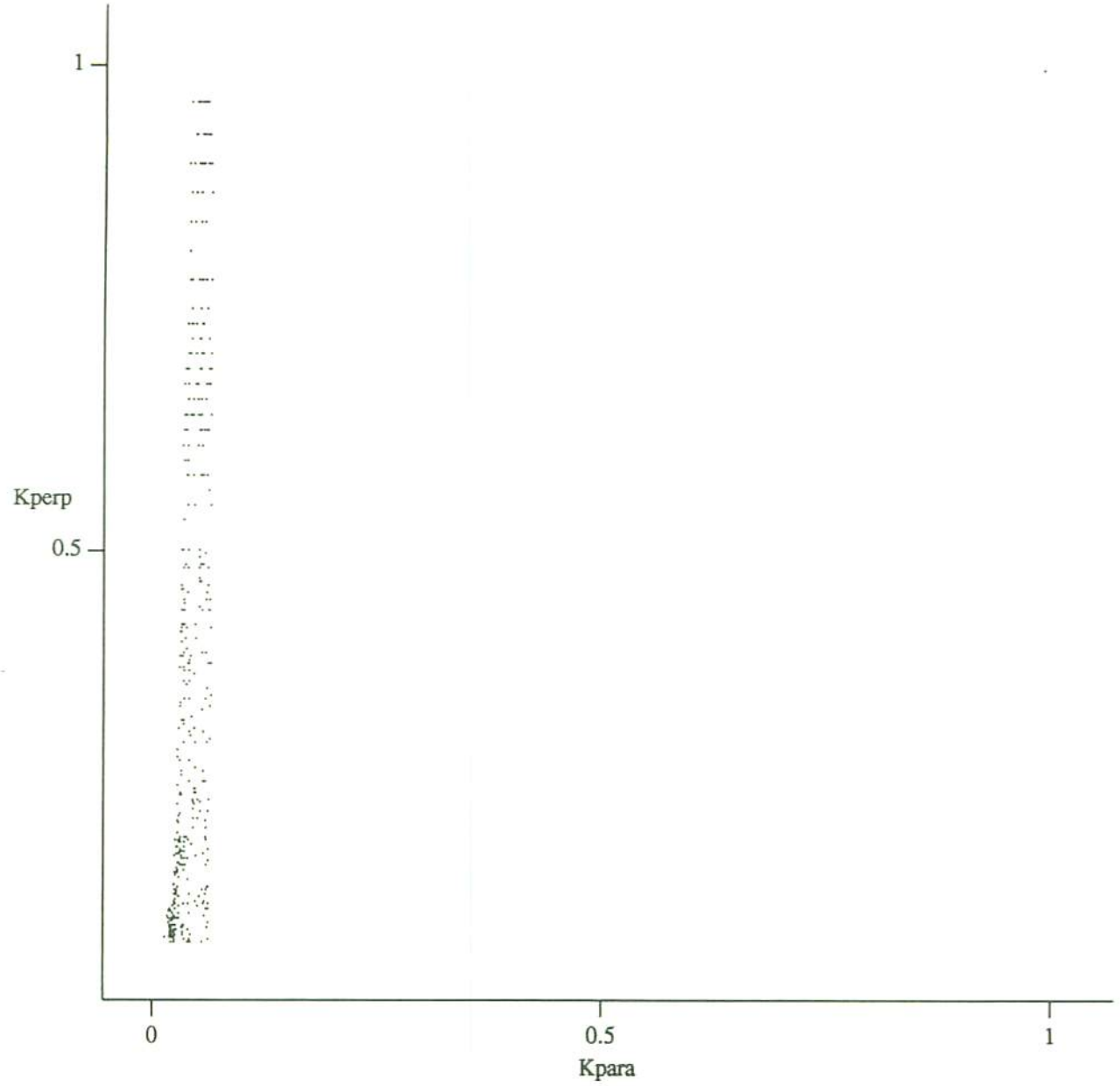

LINEARIZED Kperp vs Kpara FOR CUCS COFFEE CUP

7(b)

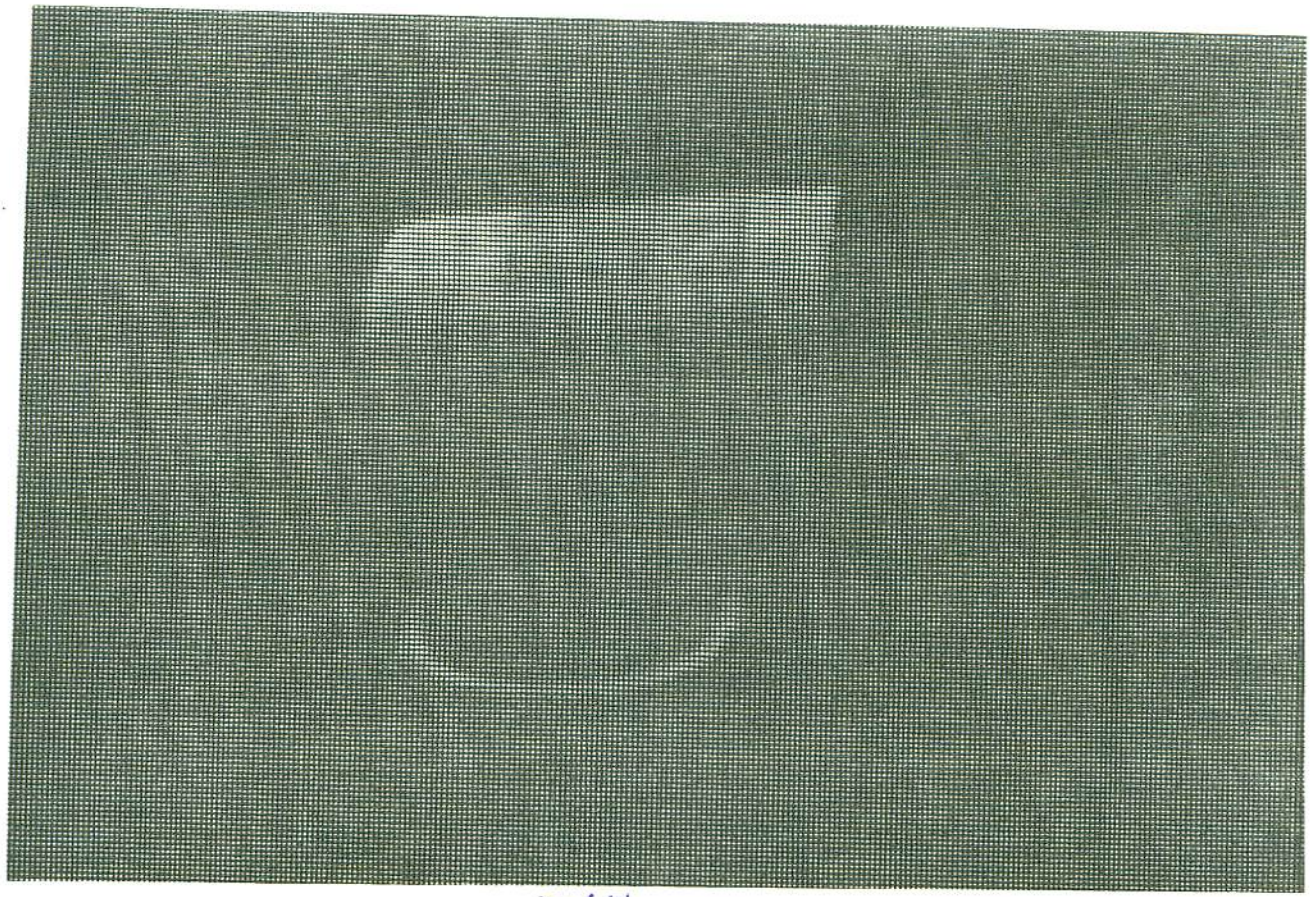

7(c)

7(d)

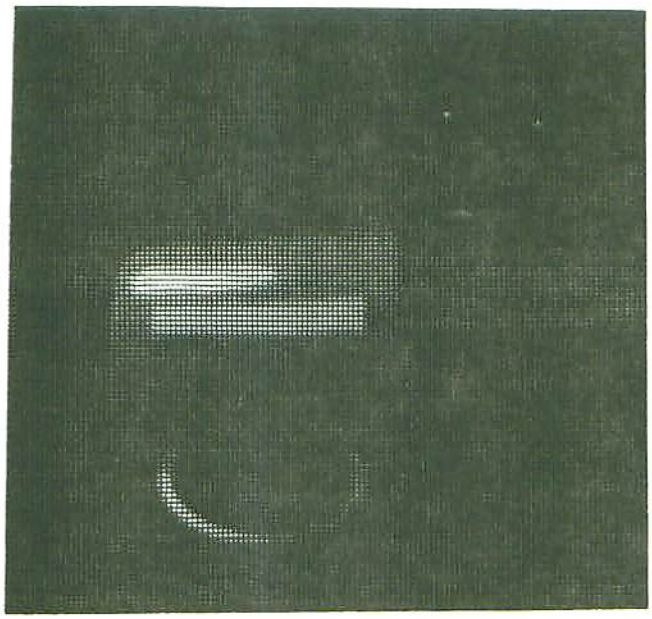

8(a)

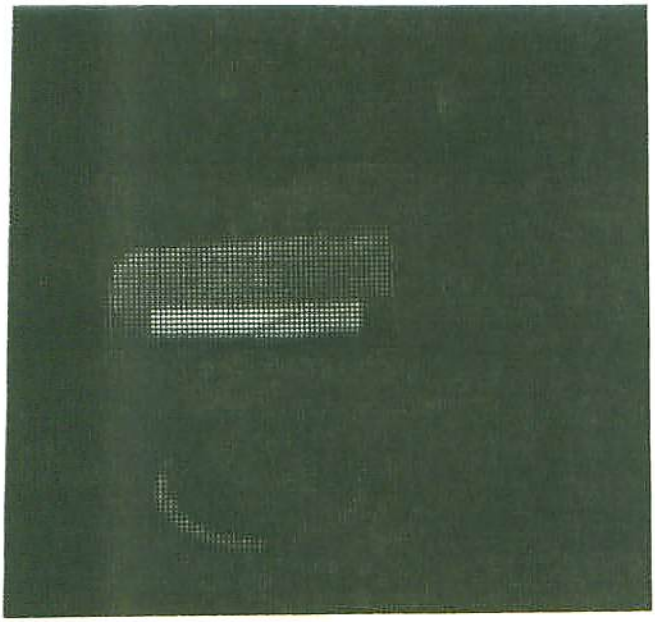

8(b)

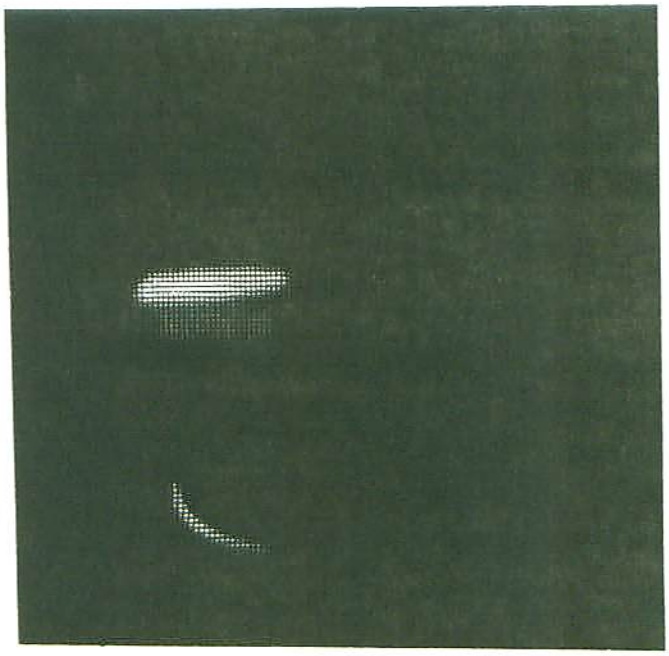

8(c)

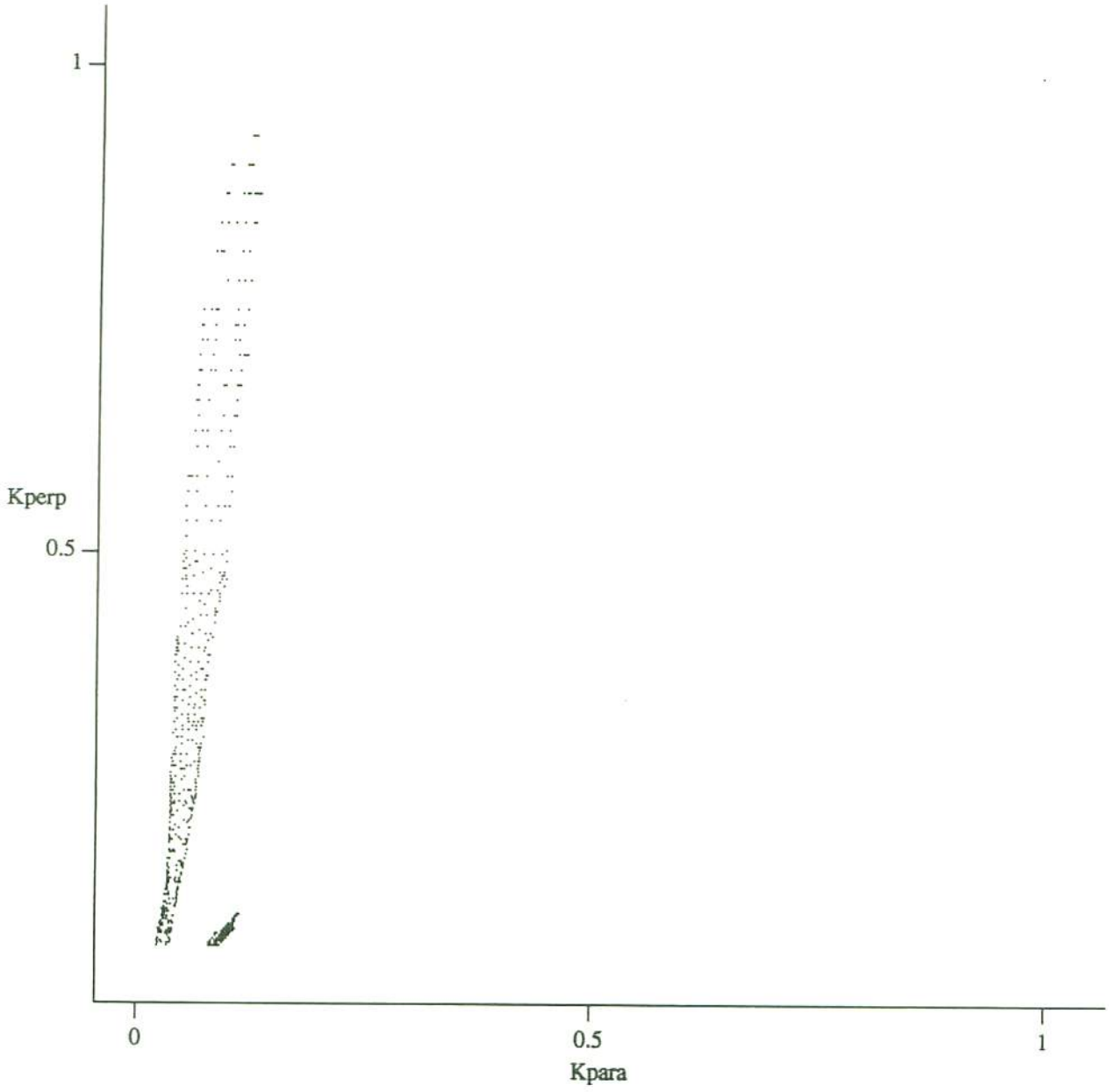

LINEARIZED Kperp vs Kpara FOR ORANGE CUP WITH WHITE STRIPE

8(d)